The Warburg Effect is the result of faster ATP production by glycolysis than respiration

Authors: Matthew A. Kukurugya[1,3], Denis V. Titov[1,2,3,*]

[1]Department of Molecular & Cell Biology, University of California, Berkeley CA, 94720
[2]Department of Nutritional Sciences & Toxicology, University of California, Berkeley CA, 94720
[3]Center for Computational Biology, University of California, Berkeley CA, 94720
*Corresponding author. Email: titov@berkeley.edu

Abstract

Many prokaryotic and eukaryotic cells choose to partially metabolize glucose to organism-specific byproducts instead of fully oxidizing it to carbon dioxide and water, even in the presence of oxygen. This phenomenon was originally observed in tumor cells and is often referred to as the Warburg Effect. The benefit to a cell has been unclear, given that partial metabolism of glucose yields an order of magnitude less ATP per molecule of glucose than complete oxidation. Here, we propose and test the hypothesis that the Warburg Effect stems from the optimization of energy metabolism that allows cells to produce ATP at the highest possible rate in the presence of excess glucose independent of cell growth rate. To test our hypothesis, we estimated the yield, specific activity, and proteome occupancy of various versions of the glycolysis and respiration pathways in three different organisms. We found that organism-specific glycolytic pathways produce ATP at a 1.1-1.5 (*E. coli*), 1.4-2.0 (*S. cerevisiae*), and 2-4.8-fold (mammalian cells) faster rate per gram of pathway protein than respective respiration pathways. For *E. coli*, only the respiro-fermentative Pta-AckA version of glycolysis, not fermentative glycolysis, produced ATP faster than respiration, explaining the preference for the Pta-AckA pathway in the presence of oxygen. We then showed that a simple mathematical model that takes these estimates as the only inputs (i.e., model has no free parameters) can accurately predict absolute rates of glycolysis byproduct secretion and respiration in *E. coli*, *S. cerevisiae*, and mammalian cells under a variety of conditions irrespective of growth rate. Taken together, our study suggests that the Warburg Effect is a manifestation by which cells optimize the rate of energy generation.

Introduction

The Warburg Effect remains one of the most well-documented, yet incompletely understood phenomena in cancer biology. In 1924, Otto Warburg made the seminal observation that *in vivo* tumors showed a preference for converting glucose to lactic acid via fermentation in the presence of oxygen instead of complete oxidation to carbon dioxide and water[1,2]. Although the initial discovery was made in tumor cells, the Warburg Effect-like metabolism has since been described for numerous proliferating cells, including acetate production through the Pta-AckA pathway in *E. coli,* ethanol fermentation in *S. cerevisiae,* and lactic acid fermentation in non-transformed mammalian cells. This phenomenon is also referred to as the Crabtree Effect in *S. cerevisiae* and "overflow metabolism" in *E. coli*. To simplify nomenclature, here, we will collectively refer to various organism-specific pathways for partial metabolism of glucose (i.e., fermentation in *E. coli*, *S. cerevisiae*, and mammalian cells and respiro-fermentative Pta-AckA acetate pathway in *E. coli*) as *glycolysis*, to organism-specific pathways for complete oxidation of glucose to carbon dioxide and water as *respiration*, and to the preference for incomplete oxidation of glucose in the presence of oxygen as *the Warburg Effect*. Respiration can yield more than an order of magnitude more ATP per molecule of glucose than glycolysis. The rationale for why cells prefer a lower ATP-yielding glycolysis and thus seemingly less efficient pathway for ATP production in the presence of oxygen has remained elusive.

Currently, no hypothesis is widely accepted to describe why the Warburg Effect occurs[3–6]. Warburg himself proposed that high glycolysis rates in cancer cells were due to an impairment in respiration[2]. However, numerous studies have since demonstrated a prominent role of respiration in ATP production during cell proliferation[7,8]. Others have proposed that the transition from respiration to glycolysis in proliferating cells could be a mechanism to limit reactive oxygen species production[9,10], to satisfy the demand for biosynthetic precursors[11,12], to regulate the $NADH:NAD^+$ redox balance[13–15], or to help yeast out-compete other microorganisms by rapidly consuming glucose[16]. Our hypothesis builds on two sets of observations. First, a trade-off between yield and rate for ATP-producing pathways has been explored in theoretical studies, highlighting the advantages of high rate over high yield ATP-producing pathways under some conditions[17,18]. Second, several studies proposed competition for limited resources as an explanation for the Warburg Effect. In *E. coli*, it has been suggested that competition for plasma membrane area drives glycolysis, where glycolysis can produce more ATP per unit of limiting membrane area[19] since glucose transporters occupy less membrane space than the respiratory chain enzymes. Several studies proposed that glycolysis might be more proteome efficient than respiration, and a switch to glycolysis allows rapidly growing cells to allocate more of their proteome to ribosomes or other enzymes required for rapid growth[20,21]. Similarly, it has also been suggested that the diversity of glycolytic pathways in prokaryotes may represent a tradeoff between ATP yield and the enzyme mass needed to support the pathway flux[22].

The current hypotheses for why the Warburg Effect occurs have three limitations that we sought to address in this study. First, the current hypotheses assume that the Warburg Effect occurs in proliferating cells while it is well known that it can occur irrespective of growth[23–26]. Second, most

of the hypotheses are specific to one organism, which limits their ability to provide a unifying explanation for its occurrence in *E. coli*, *S. cerevisiae*, and mammalian cells. Finally, none of the proposed hypotheses can quantitatively predict absolute rates of glycolysis and respiration for a diverse set of organisms and conditions as would be required for a working theory.

Here we propose and test a unifying hypothesis for the occurrence of the Warburg Effect-like metabolism in *E. coli*, *S. cerevisiae*, and mammalian cells. We propose that the Warburg Effect is the result of the optimization of energy metabolism, specifically with respect to producing ATP at a maximal rate for a given glucose availability. To test our hypothesis, we developed a mathematical model that contains only five parameters including yield and specific activity of respiration and glycolysis, and maximal proteome fraction that can be occupied by ATP-producing enzymes. We estimated the values of these five parameters from experiments (i.e., our model has no free parameters) and showed that our model can quantitatively predict the onset of the Warburg Effect, as well, glycolytic and respiration rates under various conditions in *E. coli*, *S. cerevisiae*, and mammalian cells irrespective of growth rate.

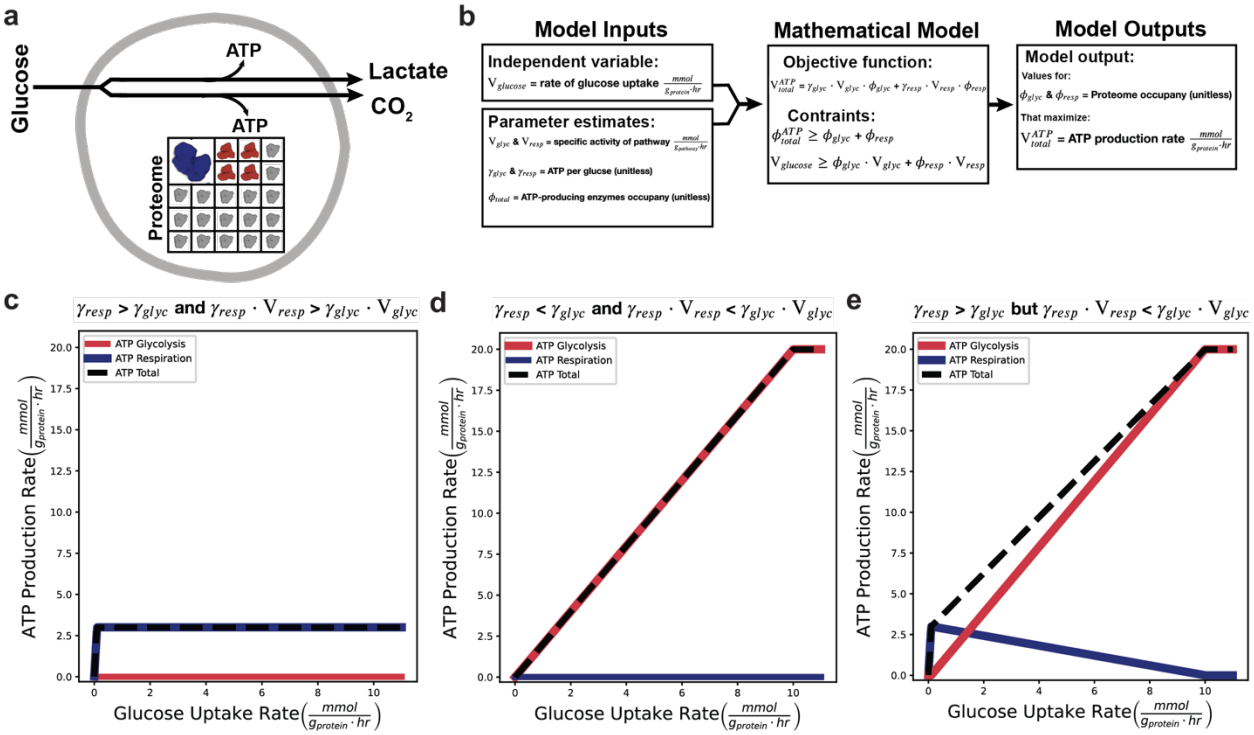

Figure 1 -- Model predicts theoretical conditions for onset of the Warburg Effect

a) Illustration of model. **b)** Overview of mathematical model. **c)** Preferred ATP-producing pathways if parameters of yield of ATP per molecule of glucose (γ) and the specific activity of ATP production ($\gamma \cdot V$) are both higher for respiration, **d)** both higher for glycolysis, **e)** or if the yield is higher for respiration ($\gamma_{resp} > \gamma_{glyc}$), but the specific activity of ATP production is higher for glycolysis ($\gamma_{resp} \cdot V_{resp} < \gamma_{glyc} \cdot V_{glyc}$). In each case, the maximal ATP production rate is represented for the dashed line.

Results

Model that maximizes ATP production rate leads to the Warburg Effect

We propose a hypothesis that the Warburg Effect results from cells switching between glycolysis and respiration to achieve maximal ATP production rates at different environmental conditions. Cells have to obey three biochemical constraints while optimizing ATP production (Fig. 1a): i) glucose and oxygen consumption are limited by glucose and oxygen availability in the surrounding media, ii) a finite fraction of proteome is dedicated to ATP-producing enzymes while the protein concentration of the cell remains constant as has been experimentally observed[27–31], and iii) the maximal ATP production rate by glycolysis or respiration pathways is limited by respective enzyme kinetics. To describe the maximal ATP production rate by respiration or glycolysis, we introduce a new metric that we call the specific activity of the pathway. We define the specific activity of the pathway as mmol of product produced (or substrate consumed) per hour by g of pathway protein by analogy with a widely used specific activity of enzymes defined as μmol product produced per min per mg of enzyme. We assume that cells are free to shift the relative rates of glycolysis and respiration through a combination of changes in the expression of enzymes and transporters, post-translational modifications, and allosteric regulation as long as the above constraints are satisfied.

To test the feasibility of our hypothesis, we constructed a mathematical model (Fig. 1b). Our aim was to keep the mathematical model as simple as possible to keep the interpretation of results straightforward. The main output of the model is the prediction of glycolysis and respiration rates that lead to maximal ATP production rate V_{total}^{ATP} with units of mmol ATP per g cellular protein per hour under the constraints described above. The V_{total}^{ATP} is a sum of the ATP production rate from glycolysis V_{glyc}^{ATP} and the ATP production rate from respiration V_{resp}^{ATP}

$$V_{total}^{ATP} = V_{glyc}^{ATP} + V_{resp}^{ATP} \tag{1}$$

The V_{glyc}^{ATP} and V_{resp}^{ATP} are the product of the specific activity of glucose consumption (V_{glyc} or V_{resp} with units of mmol glucose per g pathway protein per hour), the ATP yield per molecule of glucose (γ_{glyc} or γ_{resp}), and the fraction of the proteome that is occupied by respective pathway enzymes (ϕ_{glyc} or ϕ_{resp})

$$V_{glyc}^{ATP} = V_{glyc} \cdot \gamma_{glyc} \cdot \phi_{glyc} \tag{2}$$

$$V_{resp}^{ATP} = V_{resp} \cdot \gamma_{resp} \cdot \phi_{resp} \tag{3}$$

Substituting equations 2 and 3 into equation 1 then describes the cellular V_{total}^{ATP}, which is the objective function of the model

$$V_{total}^{ATP} = V_{glyc} \cdot \gamma_{glyc} \cdot \phi_{glyc} + V_{resp} \cdot \gamma_{resp} \cdot \phi_{resp} \tag{4}$$

The model uses linear programming to find the values of ϕ_{glyc} and ϕ_{resp} that produce maximal V_{total}^{ATP} for a given glucose uptake rate. The objective function is subject to two mathematical constraints. First, the fraction of the proteome that is occupied by the sum of glycolysis (ϕ_{ferm})

and respiration (ϕ_{resp}) enzymes must not exceed the maximal fraction of proteome dedicated to ATP-producing enzymes (ϕ_{total}^{ATP})

$$\phi_{glyc} + \phi_{resp} \leq \phi_{total}^{ATP} \quad (5)$$

Second, the sum of glucose consumption rates by glycolysis and respiration must not exceed the given maximal glucose uptake rate ($V_{max}^{glucose}$)

$$V_{glyc} \cdot \phi_{glyc} + V_{resp} \cdot \phi_{resp} \leq V_{max}^{glucose} \quad (6)$$

Our model predicts that if both the yield of ATP per molecule of glucose (γ) and the specific activity of ATP production ($V \cdot \gamma$) are higher for one pathway over another (e.g., $\gamma_{resp} > \gamma_{glyc}$ and $V_{resp} \cdot \gamma_{resp} > V_{glyc} \cdot \gamma_{glyc}$), then that pathway will be the preferred ATP-producing pathway regardless of glucose availability (Fig. 1c,d). However, if the yield of ATP per molecule of glucose is higher for respiration ($\gamma_{resp} > \gamma_{glyc}$), while the specific activity of ATP production is higher for glycolysis ($V_{glyc} \cdot \gamma_{glyc} > V_{resp} \cdot \gamma_{resp}$), then respiration produces ATP faster at low glucose uptake rates, while glycolysis produces ATP faster at high glucose uptake rates (Fig. 1e). In other words, the cell can produce ATP at the fastest rate using high yielding respiration at low glucose availability (Fig. 1e and Extended Data Fig. 1a,e), a mixture of high yielding respiration and high rate glycolysis at intermediate glucose availability (Fig. 1e and Extended Data Fig. 1b,c,f,g), or even with glycolysis alone to achieve the maximal ATP production rate (Fig. 1e and Extended Data Fig. 1d,h).

Our simple model assumes that glucose is used as the substrate for both glycolysis and respiration; however, the conclusions stay the same if a saturating concentration of a respiratory substrate other than glucose is present such as acetate, glycerol, fatty acids, or amino acids (Extended Data Fig. 2 and Supplementary Discussion 1). The latter can be intuitively understood by considering that the majority of respiratory ATP is produced by tricarboxylic acid (TCA) cycle and electron transport chain (ETC) enzymes regardless of the specific substrate, and thus, the specific activity of respiratory ATP production is similar for different substrates.

In summary, our model predicts a transition from respiration to glycolysis as the glucose uptake rates increases (i.e., the Warburg Effect) under certain combinations of yield and specific activity of glycolysis and respiration.

Glycolysis produces ATP at a faster rate than respiration

We next estimated the yields and specific activities of ATP production of glycolysis and respiration to determine if their values fall into the range where our hypothesis predicts the occurrence of the Warburg Effect (i.e. $\gamma_{resp} > \gamma_{glyc}$ and $V_{resp} \cdot \gamma_{resp} < V_{glyc} \cdot \gamma_{glyc}$). To test the general applicability of our hypothesis, we chose to focus on three organisms, *E. coli*, *S. cerevisiae*, and mammalian cells, since they span multiple kingdoms of life, exhibit Warburg Effect-like metabolic switch, have unique bioenergetic pathways, and have been extensively studied.

We first compiled the ATP yields of each pathway per molecule of glucose (Extended Data Table 2). Glycolysis yields two molecules of ATP per glucose (γ_{glyc}) for *E. coli, S. cerevisiae*, and mammalian cells. In addition to glycolysis, *E. coli* can utilize the respiro-fermentative Pta-AckA pathway[32–34] that uses glycolysis and ETC but not TCA cycle enzymes to produce acetate and carbon dioxide with a yield of 11 ATP per molecule of glucose. All three organisms have unique ATP yields per molecule of glucose for respiration (γ_{resp}) due to the variable proton pumping ability of their ETC complexes as well as the proton / ATP stoichiometry for their ATP synthases. While the maximum theoretical yield for respiration is well-known for all three organisms, the actual yield is uncertain due to the presence of the proton leak[35]. For mammalian cells, we estimated the proton leak to be 25% using the oxygen consumption data (Extended Data Table 3). The ATP yield for mammalian respiration is then 28 ATP per glucose. Due to a lack of independent estimates, we also assumed 25% proton leakage for *E. coli* and *S. cerevisiae*, yielding 24 and 20 ATP per glucose, respectively. In summary, respiration yields 12- (2.2- for Pta-AckA pathway), 10-, and 14-fold more ATP per glucose than glycolysis in *E. coli*, *S. cerevisiae*, and mammalian cells, respectively (Extended Data Fig. 4a-c).

Next, we used two orthogonal approaches to estimate whether the specific activity of ATP production for glycolysis is larger than for respiration (i.e., $V_{resp} \cdot \gamma_{resp} < V_{glyc} \cdot \gamma_{glyc}$). In the first approach, we estimated the specific activities of the pathways by summing up specific activities of individual enzymes that make up the pathway adjusted for pathway stoichiometry. We made a simplifying assumption that the k_{cat} of enzymes in glycolysis and respiration are similar so that they will cancel out when we look at the ratios of pathway specific activities. Therefore, the ratio of the specific activities of ATP production of glycolysis and respiration would be driven by differences in molecular weights of individual enzymes, pathway stoichiometries and yield of ATP per glucose.

$$\frac{\gamma_{glyc} \cdot V_{glyc}}{\gamma_{resp} \cdot V_{resp}} = \frac{\gamma_{glyc} \cdot \sum_{i=1}^{k} MW_i^{resp} \cdot Stoich_i^{resp}}{\gamma_{resp} \cdot \sum_{i=1}^{n} MW_i^{glyc} \cdot Stoich_i^{glyc}} \tag{7}$$

This approach is a conservative estimate since (1) we assumed the rates of all enzymes are equal, when the ETC complexes are typically slower than glycolytic enzymes and (2) our approach only considered the total molecular weight of core ETC proteins and does not include other mitochondrial proteins that are required for biogenesis and maintenance of mitochondria. Adjusting for slower ETC enzyme rates or adding other mitochondrial proteins would further increase the ratio of specific activity of ATP production of glycolysis to respiration.

The estimates based on the first approach show that, despite a much larger ATP yield per glucose for respiration compared to glycolysis, the molecular weight and stoichiometry of respiratory enzymes are so large that the ratio of specific activities of ATP production of glycolysis to respiration are 0.8 (1.1 for Pta-AckA pathway), 2, and 2 for *E. coli*, *S. cerevisiae*, and mammalian cells, respectively (Fig. 2a-c). Extended Data Fig. 3 illustrates the large mass and stoichiometry differential of the two ATP-producing pathways in *E. coli*, *S. cerevisiae*, and mammalian cells.

For the second approach, we used experimental data to estimate the specific activities of ATP production of glycolysis and respiration (Extended Data Fig. 4g-i). The specific activity of glucose

consumption was calculated by taking the maximal cellular glucose consumption rate by a given pathway (mmol glucose per gram of cellular protein per hr) and dividing it by the fraction of the proteome occupied by the pathway (ϕ_{glyc} or ϕ_{resp})

$$V_{glyc/resp} = \frac{Max\ cellular\ glyc/resp\ rate}{\phi_{glyc/resp}} \tag{8}$$

We determined the maximal glycolysis and respiration rates for *E. coli, S. cerevisiae*, and mammalian cells by compiling an extensive dataset from 38 independent publications containing 57 measurements of production rate of glycolysis products (i.e, acetate, ethanol, lactate) and oxygen consumption rates, which were converted to glucose consumption rate using known stoichiometry of the pathways (Extended Data Table 1). For each organism, we calculated ϕ_{glyc}, and ϕ_{resp} from proteomics data (Extended Data Fig. 4d-f; Extended Data Table 4). We made corrections to ϕ_{resp} to account for mitochondrial proteins that are required for mitochondrial biogenesis and function but are not core respiration components by including into ϕ_{resp} mitochondrial proteins whose expression was significantly ($p < 0.05$) and positively correlated ($\rho > 0$) with the sum of the TCA and ETC proteins. In addition, we corrected proteomics data for *E. coli* and *S. cerevisiae* grown in minimal media by subtracting fractions of glycolysis and the TCA cycle that are used for biosynthesis. We note that like the first approach, this estimation is conservative as membrane-bound ETC complexes are expected to be underrepresented in proteomics data. We also did not correct for the use of glycolysis and TCA cycle for biosynthesis in rich media, and we did not include all mitochondrial proteins in ϕ_{resp}. Correcting for any of these observations would further increase the ratio of specific activities of ATP production by glycolysis to respiration.

The estimates from the second approach are consistent with the first approach and show that the ratios of specific activities of ATP production of glycolysis to respiration are 0.3 (1.5 for Pta-AckA pathway), 1.4, and 4.8 for *E. coli*, *S. cerevisiae*, and mammalian cells, respectively (Fig. 2a-c). In addition to the ratios, the second approach also yielded absolute values of specific activities of ATP production (Fig. 2d-f). We note that the specific activities of ATP production increase from mammalian cells to *S. cerevisiae* to *E. coli* by over an order of magnitude for respiration and four-fold for glycolysis, suggesting that there might be an evolutionary pressure in microbes to increase the specific activity of ATP production pathways.

In summary, we used two independent approaches to show that the specific activity of ATP production by glycolysis is 0.3-0.8-fold (1.1-1.5-fold for Pta-AckA pathway), 1.4-2-fold, and 2-4.8-fold faster than respiration in *E. coli*, *S. cerevisiae*, and mammalian cells, respectively. To the best of our knowledge, these are the only estimates of the specific activities of ATP production for any organism. Previously, Basan et al. [21] estimated the ratio of specific activity of ATP production of Pta-AckA pathway vs respiration in *E. coli* (called ratio of proteome efficiencies $\varepsilon_f/\varepsilon_r$ in that study) to be 1.5, consistent with our estimate of 1.1-1.5. Our estimates for ATP yield ($\gamma_{resp} > \gamma_{glyc}$) and specific activity of ATP production ($V_{resp} \cdot \gamma_{resp} < V_{glyc} \cdot \gamma_{glyc}$) satisfied the parameter requirements in which our model predicts the switch from respiration to glycolysis for

respiro-fermentative Pta-AckA pathway in *E. coli*, and redox-neutral fermentative glycolysis in *S. cerevisiae* and mammalian cells. Importantly, our results do not predict a benefit for switching from respiration to redox-neutral fermentative glycolysis in *E. coli*. Thus, in addition to explaining why *S. cerevisiae* and mammalian cells exhibit the Warburg Effect, our hypothesis provides an explanation for why *E. coli* exclusively use the respiro-fermentative Pta-AckA pathway in the presence of oxygen and not redox-neutral fermentative glycolysis as is the case for *S. cerevisiae*, and mammalian cells.

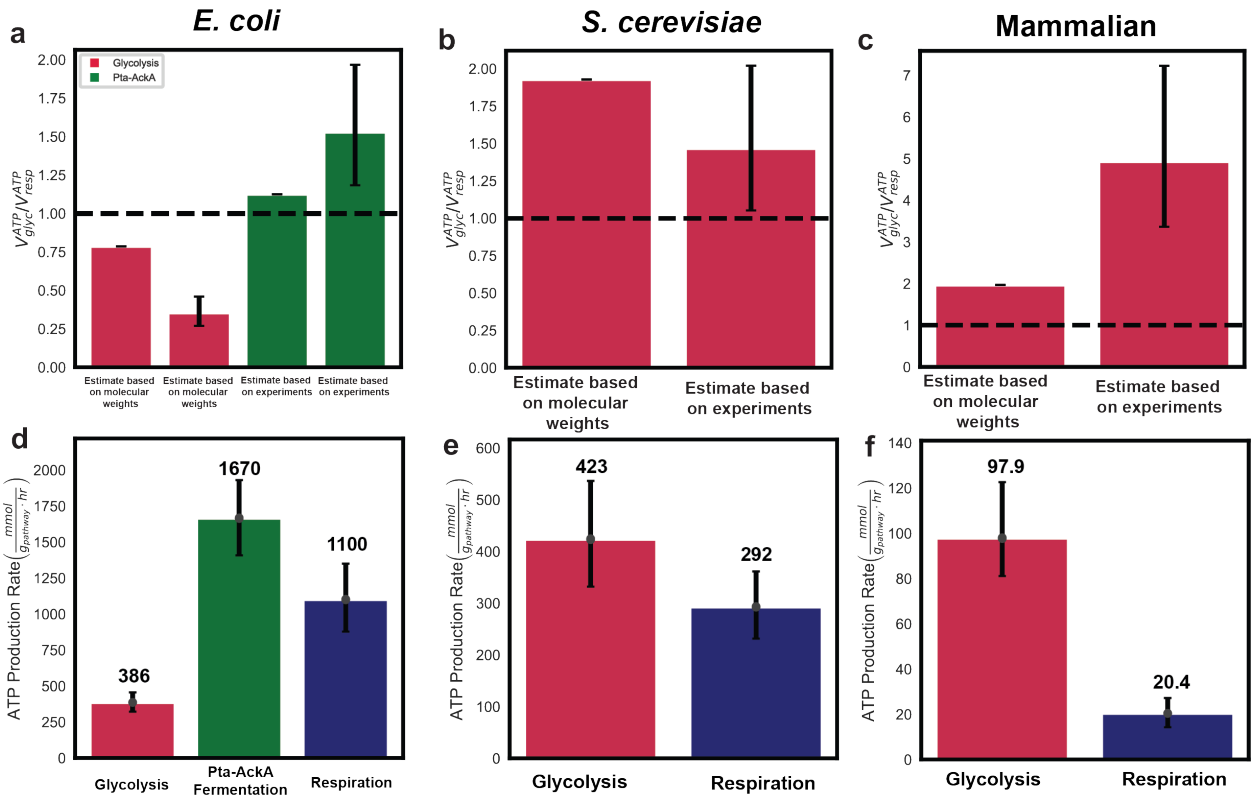

Figure 2 – Pathway-specific ATP production rates for *E. coli*, *S. cerevisiae*, and mammalian cells
a) Ratio of the maximal ATP production rate using estimates of cumulative molecular weight of the pathway or and experimental estimate of the maximal pathway rate for glycolysis (red) or the Pta-AckA pathway (green) in *E. coli*. **b,c**) Ratio of the maximal ATP production rate using estimates of cumulative molecular weight of the pathway or and experimental estimate of the maximal pathway rate for glycolysis in *S. cerevisiae* and mammalian cells, respectively. **d)** Maximal ATP production rate (mmol $g_{pathway}^{-1}$ hr^{-1}) for fermentative glycolysis (red), Pta-AckA pathway (green), and respiration (blue) for *E. coli*. **e,f)** Maximal ATP production rate (mmol $g_{pathway}^{-1}$ hr^{-1}) for fermentative glycolysis (red) and respiration (blue) for *S. cerevisiae* and mammalian cells, respectively. Error bar is the 95 percent confidence interval calculated from 10000 bootstrap iterations.

Model quantitatively predicts the onset of Warburg Effect

Having demonstrated that our hypothesis predicts the benefit of the Warburg Effect, we next tested whether our model is able to quantitatively predict the onset of the Warburg Effect as well as glycolysis and respiration rates measured under different experimental conditions in *E. coli*, *S. cerevisiae*, and mammalian cells. The additional model parameter that we needed for this test was the total fraction of the proteome dedicated to ATP-producing enzymes (ϕ_{total}) that we estimated

from proteomics data (Extended Data Fig. 4d-f). We used glucose uptake rate as the only input. For each given glucose uptake rate, the model used the four organism-specific model parameters as described in the last section (γ_{glyc}, γ_{resp}, V_{glyc}, and V_{resp}) and the total fraction of the proteome dedicated to ATP-producing enzymes (ϕ_{total}) to determine the onset of the Warburg Effect as well as the glycolysis and respiration rates that allow cells to achieve a maximal ATP production rate (Fig. 3). We have manually compiled an extensive dataset of glucose uptake, glycolysis byproduct production, and respiration rates from 29 publications containing different strains, cell types, and experimental conditions to test the general applicability of our hypothesis (Extended Data Table 5). We want to highlight three important points before describing the results: (1) Figure 3 shows the predictions of the model (shaded region or line) over experimental data (points) with no model fitting, (2) model parameters were estimated from different experiments, (3) model equations were the same across organisms and model parameters (ϕ_{total}, γ_{glyc}, γ_{resp}, V_{glyc}, and V_{resp}) for each organism were those described in the previous section, (4) our hypothesis assumes that the proteome fraction allocated to ATP-producing enzymes ϕ_{total} is a constant value as we wanted to keep our model as simple as possible, but it is known that ϕ_{total} can change under different conditions[21,36].

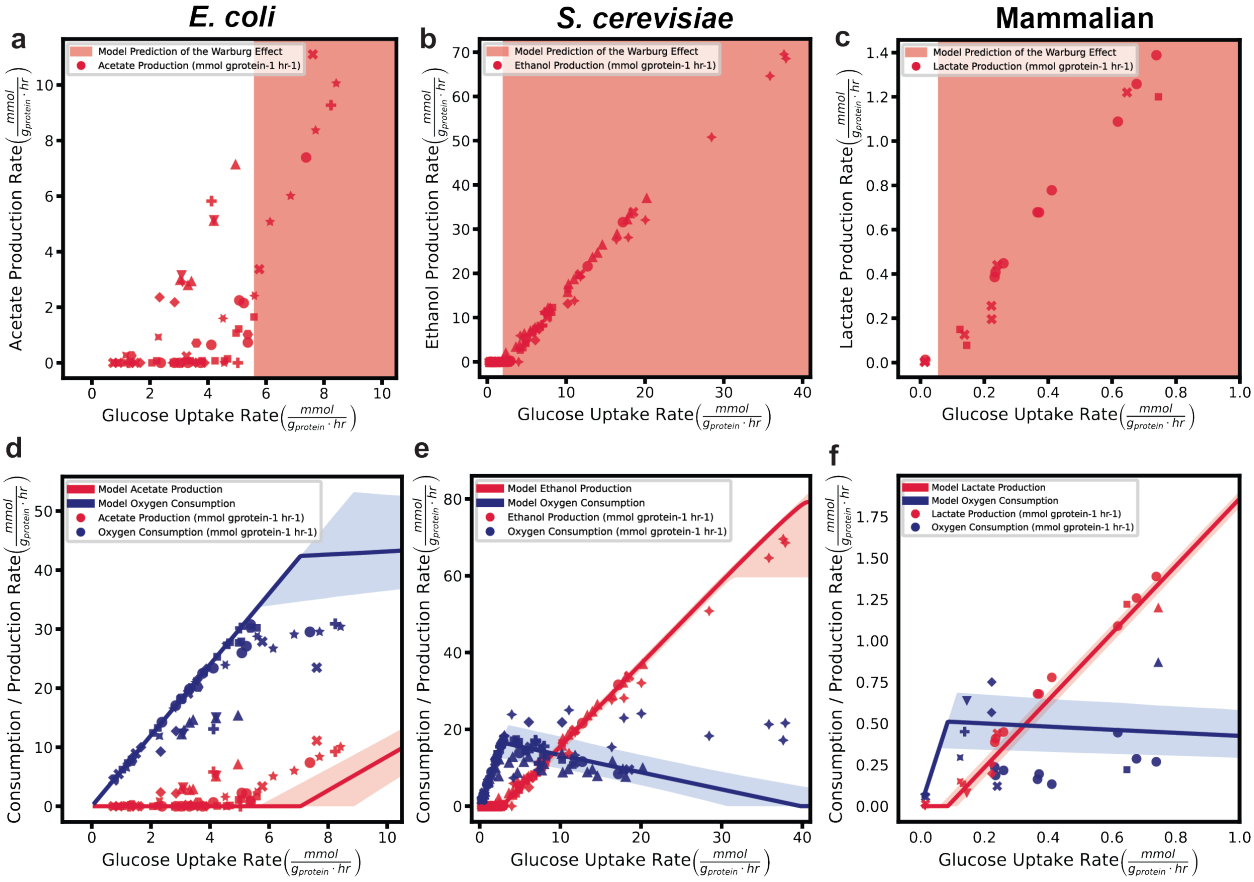

Figure 3 – Organism-specific model predictions of the Warburg Effect

a,b,c) Comparison of the model prediction (shaded region) for the glucose uptake rate in which glycolysis occurs **d,e,f)** Comparison of model predictions (lines) and experimental observations (points) for glycolysis (red) and

respiration (blue) rates of *E. coli*, *S. cerevisiae*, and mammalian cells, respectively. Note that each unique point shape represents data from a distinct publication.

Our model was able to accurately predict the glucose uptake rate range where the Warburg Effect is observed (Figure 3a-c). Furthermore, our model accurately predicted the absolute rates of acetate, ethanol, and lactate production, and oxygen consumption over a two-order of magnitude range of glucose consumption rates in *E. coli*, *S. cerevisiae,* and mammalian cells (Figure 3d-f). Most of the experimental data are within the 95% confidence interval of model predictions, especially given the experimental errors of data points not displayed here for clarity. We note that for *E. coli* our predictions of acetate production and respiration at a low glucose uptake rate were accurate, but our simple model overestimated the point where the shift to acetate production occurs by ~30%, which we speculate is due to the known decrease in the proteome fraction allocated to ATP-producing enzymes ϕ_{total} at high glucose availability[21,36]. We verified that the results for *S. cerevisiae* and mammalian cells are largely unaffected if we use only the core respiratory enzymes or the full mitochondrial proteome to estimate ϕ_{total} and V_{resp}, showing that our conclusions are independent of our assumptions about mitochondrial proteome fraction that is tied to ATP-production (Extended Data Fig. 6). The latter is in part expected as changing the mitochondrial proteome fraction that is tied to ATP production will affect the specific activity V_{resp} and the fraction of the proteome dedicated to ATP-producing enzymes ϕ_{total} in the opposite directions, thus, partially canceling each other out.

Model predicts the onset of Warburg Effect independent of growth rate

Our hypothesis proposes that glucose availability and not the growth rate is driving the onset of the Warburg Effect. To tease apart the role of growth rate and glucose availability, we have used *E. coli* and *S. cerevisiae* datasets from nitrogen, and phosphorus-limited growth conditions where glucose uptake rate and growth rate diverge significantly. In these datasets, the correlation between growth rate and glycolysis is weak ($\rho = 0.47$ and $\rho = 0.41$ for *E. coli* and *S. cerevisiae*, respectively) (Fig. 4a,b) as compared to the correlation between the glucose uptake rate and glycolysis ($\rho = 0.70$ and $\rho = 0.99$, respectively) (Fig. 4c,d). Our model accurately predicted the relationship between the glucose uptake and glycolysis rates in *S. cerevisiae* irrespective of growth rate (Fig. 4d). For *E. coli*, our model once again overestimated the shift to acetate production, which we believe is due to a known decrease in the proteome fraction allocated to ATP-producing enzymes ϕ_{total} at high glucose availability and, separately, under nitrogen-limited conditions[37] (Fig. 4b). These results suggest that, under nitrogen- and phosphorus-limited conditions in *E. coli* and *S. cerevisiae*, glycolysis is utilized as a major ATP production strategy as compared to the glucose-limited culture with the same growth rate due to the excess availability of glucose (Fig. 4c,d). A hypothesis dependent on growth rate instead of glucose availability would fail to capture this phenomenon.

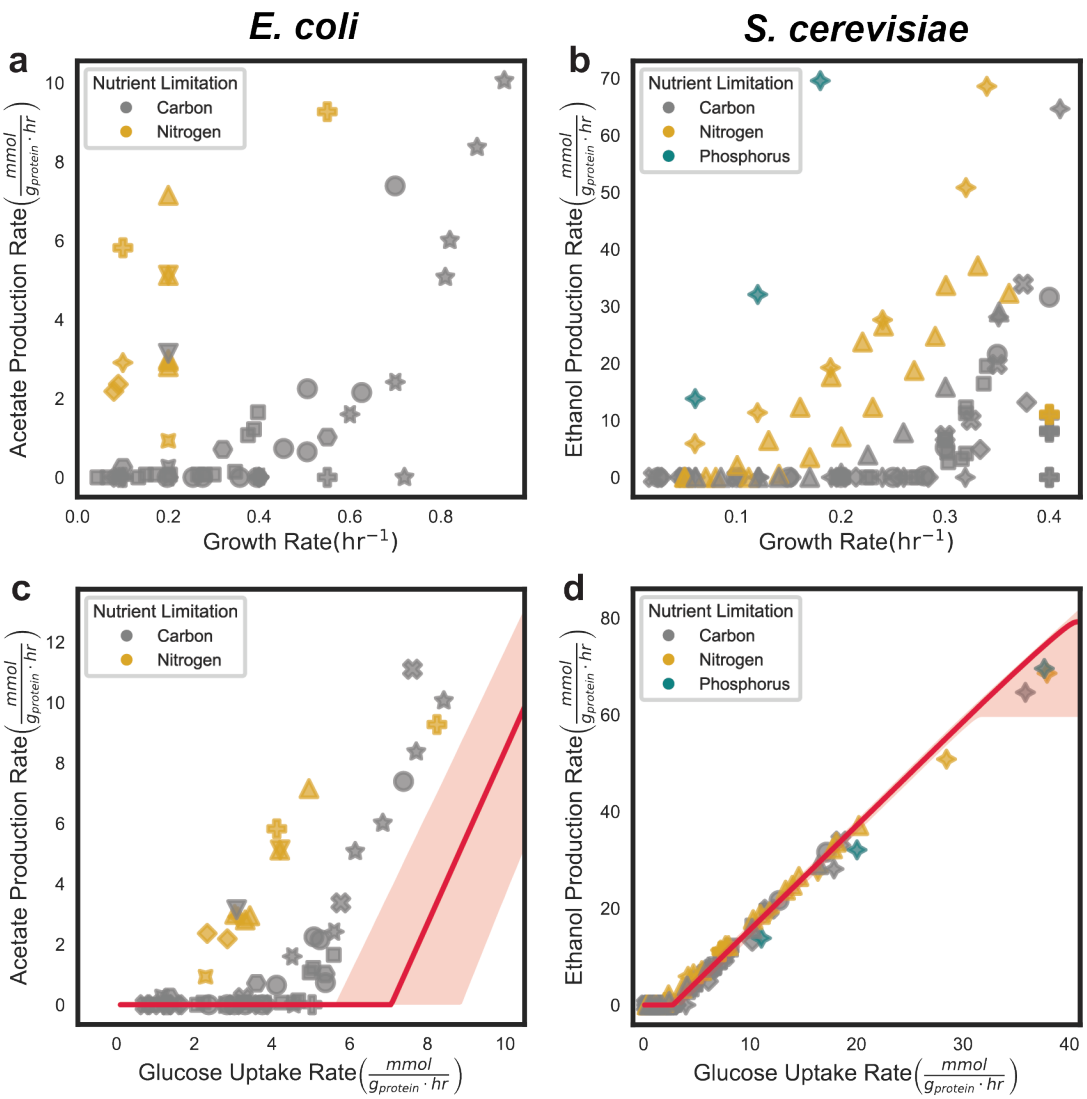

Figure 4— The Warburg Effect occurs independent of growth rate

a) *E. coli* growth rate (hr^{-1}) vs. the observed acetate production rate (mmol per g cellular protein per hr) or **b)** glucose consumption rate (mmol per g cellular protein per hr) for carbon- and nitrogen-limited cultures (grey and yellow, respectively). **c)** *S. cerevisiae* growth rate (hr^{-1}) vs. the observed ethanol production rate (mmol per g cellular protein per hr) or **d)** glucose consumption rate (mmol per g cellular protein per hr) for carbon-, nitrogen-, phosphorus-limited cultures (grey, yellow, green, respectively). Note that each unique point shape represents data from a distinct publication

Conclusion

In summary, we propose and test a hypothesis that the Warburg Effect arises from the optimization of energy metabolism in which the cell maximizes the ATP production rate for a given glucose availability. Our results suggest that while respiration has a higher yield of ATP per molecule of glucose, the ATP production rate per pathway mass is higher for Pta-AckA pathway in *E. coli*, and redox-neutral fermentative glycolysis in *S. cerevisiae*, and mammalian cells. In other words, glycolysis is more compact than respiration, which allows glycolysis to produce ATP faster than respiration when both pathways occupy the same fraction of the proteome and excess glucose is

available. Our hypothesis also explains the preferential use of the Pta-AckA pathway in *E. coli* as only the Pta-AckA pathway, and not redox-neutral fermentative glycolysis, can produce ATP at a faster rate than respiration in *E. coli*. Our conclusions are strongly supported by our mathematical model that quantitively predicted the onset of the Warburg Effect as well as absolute rates of acetate, ethanol, and lactate production, and oxygen consumption under a large range of experimental conditions in three distinct model organisms. Importantly, our model suggests that the onset of glycolysis occurs irrespective of growth, but instead due to an excess of glucose relative to the quantity that respiration can utilize. The ability of our hypothesis and corresponding model to make quantitative predictions using only five experimentally determined parameters provides a path for further validation of our hypothesis with additional experiments to improve estimates of the five model parameters and to generate more data connecting glucose uptake rate to glycolysis and respiration rates under different experimental conditions. Finally, we believe that our hypothesis can be used to explain a host of other observations beyond the Warburg Effect and Pta-AckA pathway preference, including the use of glycolysis by fast-twitch muscle cells[25,26] and the use of proton-pumping (high yield) and non-proton pumping (high rate) respiratory chain components under different conditions that is ubiquitous among microbes.

Supplementary Information is available for this paper.

Acknowledgements: This work was supported by the National Institutes of Health grant DP2 GM132933 (D.V.T.) and the University of California Cancer Research Coordinating Committee (UC CRCC) Predoctoral Fellowship (M.A.K.). We thank A. Arkin, B. Bennett, D. Botstein, A. Flamholtz, H. Garcia, R. Heald, J. Thorner, R. Wang, X. Yang and members of the Titov Lab for valuable comments on the manuscript.

Author contributions: M.A.K. and D.V.T. designed the study, analyzed the data, developed the model, and wrote the paper.

Author information: The authors declare no competing financial interests. Correspondence and requests for materials should be addressed to D.V.T. (titov@berkeley.edu).

References

1. Warburg, O., Wind, F. & Negelein, E. THE METABOLISM OF TUMORS IN THE BODY. *J. Gen. Physiol.* **8**, 519–530 (1927).
2. Warburg, O. On the origin of cancer cells. *Science* **123**, 309–314 (1956).
3. Potter, M., Newport, E. & Morten, K. J. The Warburg effect: 80 years on. *Biochem. Soc. Trans.* **44**, 1499–1505 (2016).
4. Liberti, M. V. & Locasale, J. W. The Warburg Effect: How Does it Benefit Cancer Cells? *Trends Biochem. Sci.* **41**, 211–218 (2016).
5. DeBerardinis, R. J. & Chandel, N. S. We need to talk about the Warburg effect. *Nat. Metab.* **2**, 127–129 (2020).
6. Vaupel, P. & Multhoff, G. Revisiting the Warburg effect: historical dogma versus current understanding. *J. Physiol.* **599**, 1745–1757 (2021).
7. Fan, J. *et al.* Glutamine-driven oxidative phosphorylation is a major ATP source in transformed mammalian cells in both normoxia and hypoxia. *Mol. Syst. Biol.* **9**, 712 (2013).
8. Yao, C.-H. *et al.* Mitochondrial fusion supports increased oxidative phosphorylation during cell proliferation. *eLife* **8**, e41351 (2019).
9. Brand, K. Aerobic Glycolysis by Proliferating Cells: Protection against Oxidative Stress at the Expense of Energy Yield. 10.
10. Brand, K. A. & Hermfisse, U. Aerobic glycolysis by proliferating cells: a protective strategy against reactive oxygen species1. *FASEB J.* **11**, 388–395 (1997).
11. Newsholme, E. A., Crabtree, B. & Ardawi, M. S. The role of high rates of glycolysis and glutamine utilization in rapidly dividing cells. *Biosci. Rep.* **5**, 393–400 (1985).
12. Vander Heiden, M. G., Cantley, L. C. & Thompson, C. B. Understanding the Warburg Effect: The Metabolic Requirements of Cell Proliferation. *Science* **324**, 1029–1033 (2009).

13. Dai, Z., Shestov, A. A., Lai, L. & Locasale, J. W. A Flux Balance of Glucose Metabolism Clarifies the Requirements of the Warburg Effect. *Biophys. J.* **111**, 1088–1100 (2016).
14. Luengo, A. *et al.* Increased demand for NAD+ relative to ATP drives aerobic glycolysis. *Mol. Cell* **81**, 691-707.e6 (2021).
15. Wang, Y. *et al.* Saturation of the mitochondrial NADH shuttles drives aerobic glycolysis in proliferating cells. *Mol. Cell* **82**, 3270-3283.e9 (2022).
16. Rozpędowska, E. *et al.* Parallel evolution of the make–accumulate–consume strategy in Saccharomyces and Dekkera yeasts. *Nat. Commun.* **2**, 302 (2011).
17. Pfeiffer, T., Schuster, S. & Bonhoeffer, S. Cooperation and Competition in the Evolution of ATP-Producing Pathways. *Science* **292**, 504–507 (2001).
18. Schuster, S., Pfeiffer, T. & Fell, D. A. Is maximization of molar yield in metabolic networks favoured by evolution? *J. Theor. Biol.* **252**, 497–504 (2008).
19. Szenk, M., Dill, K. A. & de Graff, A. M. R. Why Do Fast-Growing Bacteria Enter Overflow Metabolism? Testing the Membrane Real Estate Hypothesis. *Cell Syst.* **5**, 95–104 (2017).
20. Molenaar, D., van Berlo, R., de Ridder, D. & Teusink, B. Shifts in growth strategies reflect tradeoffs in cellular economics. *Mol. Syst. Biol.* **5**, 323 (2009).
21. Basan, M. *et al.* Overflow metabolism in E. coli results from efficient proteome allocation. *Nature* **528**, 99–104 (2015).
22. Flamholz, A., Noor, E., Bar-Even, A., Liebermeister, W. & Milo, R. Glycolytic strategy as a tradeoff between energy yield and protein cost. *Proc. Natl. Acad. Sci.* **110**, 10039–10044 (2013).
23. Lemons, J. M. S. *et al.* Quiescent Fibroblasts Exhibit High Metabolic Activity. *PLoS Biol.* **8**, e1000514 (2010).

24. Dong, W. *et al.* Oncogenic metabolic rewiring independent of proliferative control in human mammary epithelial cells. 2022.04.08.486845 Preprint at https://doi.org/10.1101/2022.04.08.486845 (2022).
25. Crow, M. T. & Kushmerick, M. J. Chemical energetics of slow- and fast-twitch muscles of the mouse. *J. Gen. Physiol.* **79**, 147–166 (1982).
26. Chinchore, Y., Begaj, T., Wu, D., Drokhlyansky, E. & Cepko, C. L. Glycolytic reliance promotes anabolism in photoreceptors. *eLife* **6**, e25946 (2017).
27. Dennis, P. P. & Bremer, H. Macromolecular composition during steady-state growth of Escherichia coli B-r. *J. Bacteriol.* **119**, 270–281 (1974).
28. Martínez-Salas, E., Martín, J. A. & Vicente, M. Relationship of Escherichia coli density to growth rate and cell age. *J. Bacteriol.* **147**, 97–100 (1981).
29. Marr, A. G. Growth rate of Escherichia coli. *MICROBIOL REV* **55**, 18 (1991).
30. Bosdriesz, E., Molenaar, D., Teusink, B. & Bruggeman, F. J. How fast-growing bacteria robustly tune their ribosome concentration to approximate growth-rate maximization. *FEBS J.* **282**, 2029–2044 (2015).
31. Ertugay, N. & Hamamci, H. Continuous cultivation of bakers' yeast: Change in cell composition at different dilution rates and effect of heat stress on trehalose level. *Folia Microbiol. (Praha)* **42**, 463–467 (1997).
32. Clark, D. P. The fermentation pathways of Escherichia coli. *FEMS Microbiol. Lett.* **63**, 223–234 (1989).
33. Dittrich, C. R., Vadali, R. V., Bennett, G. N. & San, K.-Y. Redistribution of Metabolic Fluxes in the Central Aerobic Metabolic Pathway of E. coli Mutant Strains with Deletion of

the ackA-pta and poxB Pathways for the Synthesis of Isoamyl Acetate. *Biotechnol. Prog.* **21**, 627–631 (2005).

34. Enjalbert, B., Millard, P., Dinclaux, M., Portais, J.-C. & Létisse, F. Acetate fluxes in Escherichia coli are determined by the thermodynamic control of the Pta-AckA pathway. *Sci. Rep.* **7**, 42135 (2017).
35. Divakaruni, A. S. & Brand, M. D. The Regulation and Physiology of Mitochondrial Proton Leak. *Physiology* **26**, 192–205 (2011).
36. Erickson, D. W. *et al.* A global resource allocation strategy governs growth transition kinetics of Escherichia coli. *Nature* **551**, 119–123 (2017).
37. You, C. *et al.* Coordination of bacterial proteome with metabolism by cyclic AMP signalling. *Nature* **500**, 301–306 (2013).
38. Wiśniewski, J. R. *et al.* Extensive quantitative remodeling of the proteome between normal colon tissue and adenocarcinoma. *Mol. Syst. Biol.* **8**, 611 (2012).
39. Wiśniewski, J. R., Hein, M. Y., Cox, J. & Mann, M. A "Proteomic Ruler" for Protein Copy Number and Concentration Estimation without Spike-in Standards *. *Mol. Cell. Proteomics* **13**, 3497–3506 (2014).